

## The Modular Nature of All-Ferrous Edge-Bridged Double Cubanes

Mrinmoy Chakrabarti,<sup>†</sup> Liang Deng,<sup>‡</sup> R. H. Holm,<sup>‡</sup> Eckard Münck,<sup>†</sup> and Emile L. Bominaar<sup>\*,†</sup>

<sup>†</sup>Department of Chemistry, Carnegie Mellon University, 4400 Fifth Avenue, Pittsburgh, Pennsylvania 15213 and

<sup>‡</sup>Department of Chemistry and Chemical Biology, Harvard University, Cambridge, Massachusetts 02138

Received October 15, 2009

Two all-ferrous, edge-bridged 8Fe–8S clusters, one capped with carbenes (**2**) and the other with phosphenes (**3**), have been characterized by <sup>57</sup>Fe Mössbauer spectroscopy. The clusters have diamagnetic ground states that yield spectra consisting of one quadrupole doublet with a large splitting (25% of absorption) and one (**3**) or two (**2**) doublets with much smaller splittings (75% of absorption). These patterns closely resemble those observed for all-ferrous 4Fe–4S clusters. Structurally, the 4Fe–4S fragments of **2** and **3** are remarkably similar to all-ferrous 4Fe–4S clusters, sharing with them the characteristic 3:1 pattern of the iron sites, a differentiation that has been shown previously to reflect spontaneous distortions of the cluster core. These spectroscopic and geometric similarities suggest that the diamagnetic ground state of the 8Fe–8S cluster results from antiferromagnetic exchange coupling of two identical 4Fe–4S modules, each carrying spin  $S_{4\text{Fe}} = 4$ . The iron atoms with the largest quadrupole splittings are located at the opposite ends of the body diagonal containing the bridging sulfides.

### Introduction

Iron–sulfur clusters have paramagnetic sites, commonly high-spin ( $S_i = 2$ ) Fe<sup>II</sup> or high-spin ( $S_i = 5/2$ ) Fe<sup>III</sup>.<sup>1,2</sup> The spin states of Fe–S clusters have been described with an effective Hamiltonian of the form  $\sum J_{ij} S_i \cdot S_j$ , representing the exchange couplings between the paramagnetic sites, amended with terms for spin-dependent resonance interaction and vibronic coupling in the case of mixed valency.<sup>3–5</sup> The combination of these interactions has the effect of composing the local spins,  $S_i$ , into specific patterns to yield the total spin ( $S$ ) state of the cluster. The spin-ordering patterns have been determined for a number of paramagnetic ( $S > 0$ ) Fe–S clusters by <sup>57</sup>Fe Mössbauer spectroscopy, which is currently the most suitable technique available for this task.<sup>6,7</sup> These analyses take advantage of the technique's ability to identify for paramagnetic cluster states the spin orientations of the individual iron sites relative to the applied magnetic field, and they have provided the spin orderings for [3Fe–4S]<sup>0</sup> ( $S = 2$ ),<sup>6</sup>

[4Fe–4S]<sup>3+</sup> ( $S = 1/2$ ),<sup>7</sup> and [4Fe–4S]<sup>1+</sup> ( $S = 1/2$ )<sup>8,9</sup> clusters. Mössbauer spectroscopy has also been successfully applied to the determination of the spin ordering in the diamagnetic ( $S = 0$ ) [4Fe–4S]<sup>2+</sup> clusters in sulfite reductase,<sup>10</sup> acetyl CoA synthase,<sup>11</sup> and [FeFe] hydrogenases,<sup>12</sup> by analyzing the internal magnetic hyperfine interactions induced at the cluster sites by one or more paramagnetic metal ions covalently linked, through a cysteinyl sulfur, to the Fe–S cluster. The Mössbauer information about the magnetic hyperfine interactions at the irons in higher nuclearity clusters, including FeMo cofactor (7Fe)<sup>13,14</sup> and the P cluster (8Fe)<sup>15</sup> of nitrogenase, have been used to propose detailed spin-ordering patterns for these clusters.

In this contribution, we address the geometry and spin ordering in two all-ferrous, edge-bridged double cubanes, complexes **2** and **3**, each containing eight Fe<sup>II</sup> sites but capped with different ligands (Figure 1).<sup>16</sup> The two 8Fe clusters are diamagnetic ( $S = 0$ , see the Results and Discussion), excluding an assessment of their spin orderings on the basis of the

\*To whom correspondence should be addressed. E-mail: eb7g@andrew.cmu.edu.

- (1) Beinert, H.; Holm, R. H.; Münck, E. *Science* **1997**, *277*, 653.
- (2) Holm, R. H.; Kennepohl, P.; Solomon, E. I. *Chem. Rev.* **1996**, *96*, 2239.
- (3) Borshch, S. A.; Bominaar, E. L.; Blondin, G.; Girerd, J.-J. *J. Am. Chem. Soc.* **1993**, *115*, 5155.
- (4) Bominaar, E. L.; Borshch, S. A.; Girerd, J.-J. *J. Am. Chem. Soc.* **1994**, *116*, 5362.
- (5) Bominaar, E. L.; Hu, Z.; Münck, E.; Girerd, J.-J.; Borshch, S. A. *J. Am. Chem. Soc.* **1995**, *117*, 6976.
- (6) Papaefthymiou, V.; Girerd, J.-J.; Moura, I.; Moura, J. J. G.; Münck, E. *J. Am. Chem. Soc.* **1987**, *109*, 4703.
- (7) Papaefthymiou, V.; Millar, M. M.; Münck, E. *Inorg. Chem.* **1986**, *25*, 3010.
- (8) Lindahl, P. A.; Day, E. P.; Kent, T. A.; Orme-Johnson, W. H.; Münck, E. *J. Biol. Chem.* **1985**, *260*, 11160.

- (9) Noodleman, L. *Inorg. Chem.* **1991**, *30*, 256.
- (10) Christner, J. A.; Münck, E.; Kent, T.; Janick, P. A.; Salerno, J. C.; Siegel, L. M. *J. Am. Chem. Soc.* **1984**, *106*, 6786.
- (11) Xia, J.; Hu, Z.; Popescu, C. V.; Lindahl, P. A.; Münck, E. *J. Am. Chem. Soc.* **1997**, *119*, 8301.
- (12) (a) Popescu, C. V.; Münck, E. *J. Am. Chem. Soc.* **1999**, *121*, 7877.
- (b) Münck, E.; Popescu, C. V. *Hyperfine Interact.* **2000**, *126*, 59.
- (13) Vrajmasu, V. V.; Münck, E.; Bominaar, E. L. *Inorg. Chem.* **2003**, *42*, 5974.
- (14) Lovell, T.; Li, J.; Liu, T.; Case, D. A.; Noodleman, L. *J. Am. Chem. Soc.* **2001**, *123*, 12392.
- (15) Mouesca, J. M.; Noodleman, L.; Case, D. A. *Inorg. Chem.* **1994**, *33*, 4819.
- (16) Deng, L.; Holm, R. H. *J. Am. Chem. Soc.* **2008**, *130*, 9878.

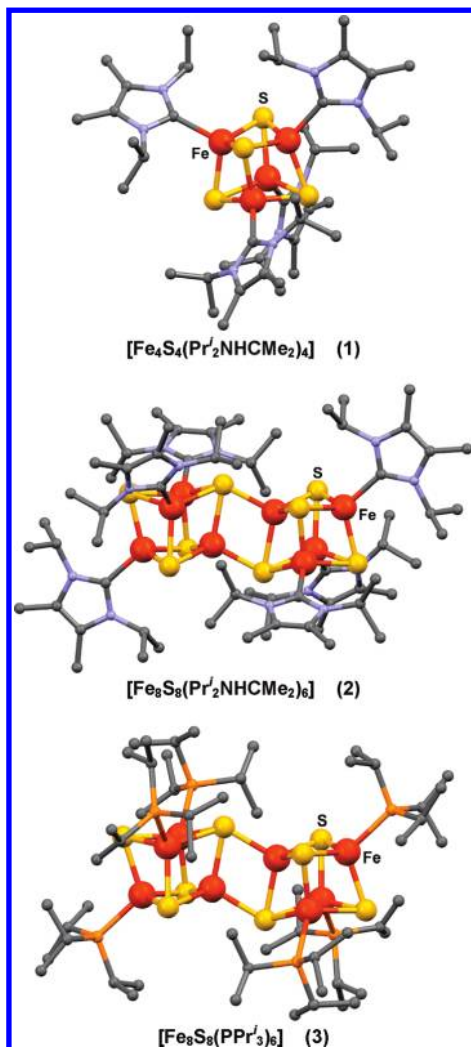


**Figure 1.** Structures of carbene-ligated single cubane **1** and the carbene- and phosphine-ligated edge-bridged double cubanes **2** and **3**, respectively. The isostructural and essentially isometric  $[\text{Fe}_8\text{S}_8]^0$  cores of the latter clusters are centrosymmetric with idealized  $C_{2h}$  symmetry.

magnetic hyperfine interactions, which vanish for  $S = 0$ . Recently, we performed a spectroscopic and theoretical analysis of the carbene-capped, all-ferrous  $[\text{4Fe-4S}]^0$  cluster ( $S = 4$ ), complex **1**, in which we established an intricate relationship between the Mössbauer properties, geometry, and spin ordering, rooted in the dependence of the exchange interactions on the structure of the  $[\text{4Fe-4S}]$  core of **1**.<sup>17,18</sup> On the basis of this understanding, we present here an analysis of the 8Fe complexes **2** and **3**.

Edge-bridged  $[\text{8Fe-8S}]$  clusters were first prepared in 1995–96.<sup>19,20</sup> Thereafter, phosphine cluster **3** was reported<sup>21</sup> and most recently the carbene cluster **2**.<sup>16</sup> Mössbauer spectra were briefly described, but the spectra were not fully assigned to specific iron sites and the origin of the diamagnetic ground state was not explained. These issues are addressed in this work.

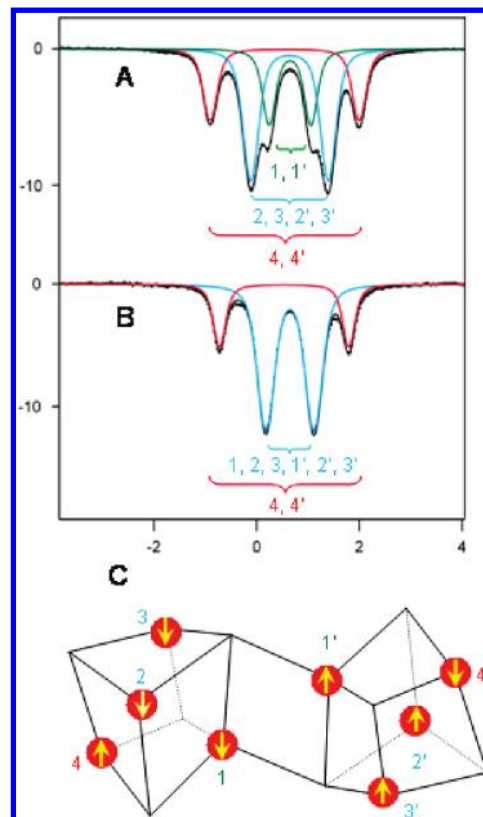


**Figure 2.** Mössbauer spectra of all-ferrous 8Fe complexes **2** (A) and **3** (B) recorded at 4.2 K without applied magnetic field. The quadrupole doublets composing the spectra are shown as colored traces and have the parameter values listed in Table 4. (C) Cartoon of  $[\text{8Fe-8S}]^0$  core in complexes **2** and **3** with the definition of the labels that identify the quadrupole doublets in the top panel with particular iron sites of the cluster (see text). The arrows indicate the ordering of the iron spins for the  $S = 0$  ground state.

## Results and Discussion

We have studied polycrystalline samples of **2** and **3** with Mössbauer spectroscopy between 4.2 and 120 K in applied fields up to 8.0 T. The 4.2 K, zero-field spectra of the carbene complex, **2**, reveal three doublets with an absorption ratio of 1:2:1 (Figure 2A), while those for **3** show two doublets with a 1:3 ratio (Figure 2B). The observed patterns can be readily understood by reference to the all-ferrous  $[\text{4Fe-4S}]^0$  cluster of **1**.<sup>17</sup> The results of ref 17 can be summarized as follows: (i) The  $[\text{4Fe-4S}]^0$  cluster contains three virtually equivalent iron sites ( $\text{Fe}_1$ ,  $\text{Fe}_2$ ,  $\text{Fe}_3$ ) whose (local)  $S_i = 2$  spins are aligned parallel to the cluster spin  $S = 4$ , and a unique iron (labeled  $\text{Fe}_4$ ) with antiparallel local spin. A similar type of spin state has recently been proposed for two  $[\text{4Co}^{\text{II}}-4\text{S}]^0$  clusters on the basis of the  $S = 3$  ground states deduced from magnetic susceptibility measurements.<sup>22</sup> (ii) The unique iron is structurally distinct from the equivalent irons. Tables 1–3 compare the two types of iron based on various geometrical features. Table 1 shows that the diagonal  $\text{Fe}\cdots\text{S}$  distance for the unique iron in **1** is 0.16 Å longer than for the equivalent sites. Moreover, Table 2 reveals that the  $\text{Fe}\cdots\text{Fe}$  distances of the unique iron to the equivalent irons are, on average, 0.1 Å longer than the distances between the equivalent irons. Accordingly, Table 3 illustrates that the  $\text{Fe-S-Fe}$  angles

(17) Chakrabarti, M.; Deng, L.; Holm, R. H.; Münck, E. *Inorg. Chem.* **2009**, *48*, 2735.

(18) Münck, E.; Bominaar, E. L. *Science* **2008**, *315*, 835.

(19) Cai, L.; Segal, B. M.; Long, J. R.; Scott, M. J.; Holm, R. H. *J. Am. Chem. Soc.* **1995**, *117*, 8863.

(20) Goh, C.; Segal, B. M.; Huang, J.; Long, J. R.; Holm, R. H. *J. Am. Chem. Soc.* **1996**, *118*, 11844.

(21) Zhou, H.-C.; Holm, R. H. *Inorg. Chem.* **2003**, *42*, 11.

(22) Deng, L.; Bill, E.; Wieghardt, K.; Holm, R. H. *J. Am. Chem. Soc.* **2009**, *131*, 11213.

**Table 1.** Average Diagonal Fe...S Distances (Å)

Fe <sub>i</sub> ...S <sub>i</sub>	1	2	3
<i>i</i> < 4	3.887	3.861	3.841
<i>i</i> = 4	4.055	4.158	4.115

**Table 2.** Average Fe...Fe Distances (Å)

Fe <sub>i</sub> ...Fe <sub>j</sub>	1	2	3
<i>i</i> = 4, <i>j</i> < 4	2.731	2.764	2.708
<i>i</i> < <i>j</i> < 4	2.629	2.622	2.592

**Table 3.** Average Fe–S–Fe Bond Angles (deg)

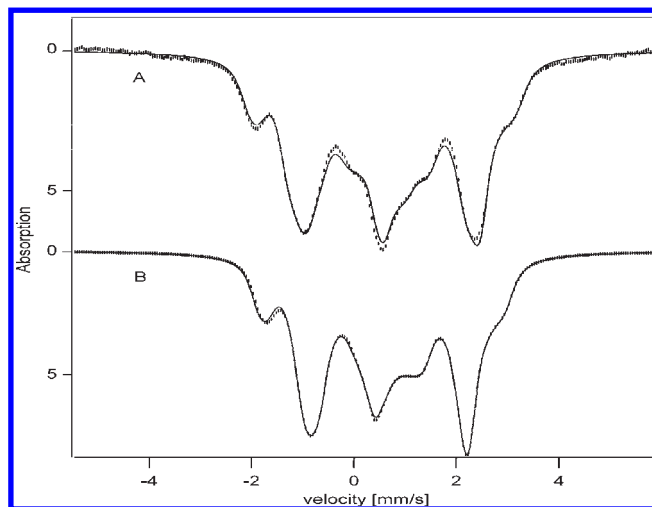
Fe <sub>i</sub> –S–Fe <sub>j</sub>	1	2	3
<i>i</i> = 4, <i>j</i> < 4	72.0	73.4	72.2
<i>i</i> < <i>j</i> < 4	68.4	67.7	67.1
<i>i</i> = 1, <i>j</i> = 1'		74.3	71.7

**Table 4.** Isomeric Shift, Quadrupole Splitting, and Asymmetry Parameter

site <sup>a</sup>	δ (mm/s)			ΔE <sub>Q</sub> (mm/s)			η		
	1 <sup>b</sup>	2	3	1 <sup>b</sup>	2	3	1 <sup>b</sup>	2	3
1	0.61	0.64	0.65	-1.6	-0.82	-0.94	0	0	0.12
2 and 3	0.62	0.64	0.65	-1.5	-1.5	-0.94	0.1	0.1	0.12
4	0.54	0.54	0.54	2.96	2.93	2.53	0.59	0.59	0.67

<sup>a</sup> Labels 1, 2, and 3 in 4Fe cluster **1** are used to distinguish between the three "equivalent" sites, based on small differences in the parameter values; the site labels for the 8Fe clusters **2** and **3** indicate specific positions in the cluster, as defined in Figure 2C. <sup>b</sup> Data taken from ref 17.

in **1** involving the unique iron are 3.5° larger than the averaged angles of the Fe–S–Fe bonds between the equivalent irons. (iii) The quadrupole splitting, ΔE<sub>Q</sub>, and isomer shift, δ, for the unique iron are distinct from those for the equivalent sites. The values of the parameters for **1**, listed in Table 4, reveal that δ and ΔE<sub>Q</sub> for the unique iron are, respectively, 0.07 mm/s smaller and 1.5 mm/s larger than for the equivalent irons. (iv) The trends described under i–iii are an intrinsic property of the 4Fe–4S core and are only weakly affected by the terminal ligands. This conclusion is based on both the remarkable similarities in the geometries and hyperfine interactions of the all-ferrous clusters in the Fe protein of nitrogenase (cysteine coordinated)<sup>23</sup> and complex **1** (carbene coordinated)<sup>17</sup> as well as on theoretical analysis that suggests that spontaneous distortions of the core give rise to these properties.<sup>17</sup> Taking into consideration point iv, we expect that the all-ferrous subcubanes in **2** and **3** resemble the all-ferrous cluster of **1**. A comparison of the geometric and hyperfine properties listed in Tables 1–4 for complexes **2** and **3** with those for complex **1** reveal that the expected similarity is indeed borne out by the data. Thus, the geometric data in Tables 1–3 show that the iron atoms in the cubane fragments with the largest quadrupole splittings and smallest isomer shifts can be unambiguously assigned to atoms Fe<sub>4</sub> and Fe<sub>4'</sub> that are located at the opposite ends of the body diagonals containing the bridging sulfides (Figure 2C). Fe<sub>4</sub> and Fe<sub>4'</sub> are indistinguishable in the spectra and represent 25% of the total absorption, consistent with the intensity observed for the quadrupole doublets displayed in red in Figures 2A and 2B. Comparison of the quadrupole splittings for the unique sites in **2** and **3** (Table 4) reveals a

**Figure 3.** The 4.2 K Mössbauer spectra of complexes **2** (A) and **3** (B) recorded in an 8.0 T field applied parallel to the  $\gamma$  beam. The solid lines are simulations for  $S = 0$  using the parameters quoted in Table 4.

weak influence of the difference in terminal ligation on this quantity. The equivalent irons (labeled 1–3 and 1'–3' in Figure 2C) are indistinguishable in **3** (Table 4) and give rise to the inner doublet of Figure 2B, accounting for 75% of the absorption. The ΔE<sub>Q</sub> and δ values for **2** (see Table 4) exhibit some site differentiation between the six equivalent sites: there are two inner doublets, with a 2:1 absorption ratio (Figure 2A), with slightly different hyperfine parameters. This ratio is consistent with an assignment which maps the inner doublet of Figure 2A to the bridging irons (1 and 1' in Figure 2C) and the middle doublet to the nonbridging, nonunique irons (2 and 3, 2' and 3' in Figure 2C). Although this assignment is probably correct, we would also like to point out that the equivalent sites in **1** show already some degree of differentiation in their hyperfine parameters in spite of having a uniform ligation.<sup>17</sup>

Given the remarkable similarity between the cubane modules of **1**, **2**, and **3**, it is reasonable to assume that the 3:1 spin ordering described for **1** is also present in the cubane modules of the two double cubanes (see Figure 2C). The remaining question at this juncture concerns the relative alignment of the spins of the two cubane modules. The 3:1 spin ordering in **1** requires that the unique iron is coupled to the three equivalent irons through antiferromagnetic exchange-coupling constants ( $J_{i4} > 0$ ,  $i = 1-3$ ) and that the three equivalent irons are mutually linked by either weak antiferromagnetic exchange or ferromagnetic exchange. In ref 17, we have argued that the differences in the  $J$  values in **1** are due to the differences in the superexchange interactions through the Fe–S–Fe bonds caused by variations in the bond angle. Thus, Fe<sub>i</sub>–S–Fe<sub>4</sub> ≈ 72° (Table 3) gives rise to antiferromagnetic exchange and Fe<sub>i</sub>–S–Fe<sub>j</sub> ≈ 68° (Table 3) to weak antiferromagnetic exchange or ferromagnetic exchange. With this criterion at hand, we now consider the exchange-coupling constants between the cubane modules in **2** and **3**. The coupling  $J_{11'}$  is mediated by two Fe–S–Fe bridges (Figure 2C) with angles of ~73° (Table 3) and, therefore, qualifies as antiferromagnetic. The couplings  $J_{12'}$ ,  $J_{13'}$ ,  $J_{21'}$ , and  $J_{31'}$  all proceed through a sulfur bridge with an angle of about 120° and are expected to be antiferromagnetic as well. The spin pattern presented in Figure 2C is consistent with the antiferromagnetic character inferred for the six intercubane

(23) Yoo, S. J.; Angove, H. C.; Burgess, B. K.; Hendrich, M. K.; Münck, E. *J. Am. Chem. Soc.* **1999**, *121*, 2534.

exchange couplings and is free of spin frustration. The overall spin of the pattern in Figure 2C is zero ( $S = 0$ ). This prediction is in agreement with the diamagnetic nature of the ground states for **2** and **3** deduced from the Mössbauer spectra recorded in applied magnetic fields (Figure 3). We do not know whether the spins of the cubane modules ( $S_{\text{cub}} = 4$ ) in **2** and **3** are good quantum numbers and to what extent the ground state has a fractional parentage to coupling schemes in which spins belonging to different modules are coupled first. Answering this question requires information about the relative magnitudes of the intra- and intercubane exchange-coupling constants,  $J_{ij}/J_{ij'}$ . Although this information is not available, we note that the intercubane exchange couplings are mediated by the bridging sulfides, which are coordinated to four irons, in contrast with the nonbridging sulfides, which are three-coordinate. The higher coordination number of the former may make it a less effective superexchange mediator, which would lend support to the notion that the modular spins ( $S_{\text{cub}} = 4$ ) are good quantum numbers.

The analysis presented here has established the modular nature of the all-ferrous double cubanes in **2** and **3** in terms of their cubane building blocks. As anticipated from our study of **1**, the geometric/electronic structure of all-ferrous, edge-bridged double cubanes is only weakly affected by changes in terminal ligation, corroborating the notion that it is an intrinsic property of the  $[8\text{Fe}-8\text{S}]^0$  core. The proposed spin ordering (Figure 2C) is up for experimental verification. Magnetic Mössbauer spectroscopy could be helpful in this respect provided one succeeds in magnetizing the cluster by linking one of its irons to an external paramagnetic site.

**Acknowledgment.** This research was supported at Carnegie Mellon University by NIH Grant GM 22701 and at Harvard University by NIH Grant GM 28856.

**Supporting Information Available:** The Fe–S–Fe bond angles (Table S1), Fe···Fe distances (Table S2), and diagonal Fe···S distances (Table S3) of complexes **2** and **3**. This material is available free of charge via the Internet at <http://pubs.acs.org>.